Mechanical Properties of Pineapple Leaf Fiber Reinforced Epoxy Composite

Sundarasetty Harishbabu,[a] Abdullah A. Elfar,[b] P. S. Rama Sreekanth ,[a] Santosh Kumar Sahu,[a,*] It Ee Lee,[c,d,*] Eng Eng Ngu,[c,e] and Borhen Louhichi [f]

The fabrication and mechanical properties of pineapple leaf fiber (PALF)–reinforced epoxy composites were evaluated with fiber loadings of 0, 5, 10, 20, and 30 wt%. Tensile and flexural properties were experimentally evaluated and validated using a finite element based Representative Volume Element (RVE) modelling approach. The results demonstrate that PALF incorporation significantly enhanced the mechanical performance of the epoxy matrix, with the 30 wt% PALF composite exhibiting maximum improvements in tensile strength (167%), Young's modulus (24%), and flexural strength (143%) relative to neat epoxy. The RVE model successfully predicted the elastic modulus, showing close agreement with experimental results and classical micromechanical models, including the Rule of Mixtures and Mori–Tanaka formulations. In addition, Finite Element Analysis (FEA) predictions of tensile and flexural strengths deviated by less than 10% from experimental values, confirming the robustness of the numerical framework. The integrated experimental–numerical methodology presented in this work provides a reliable basis for the design and assessment of sustainable PALF–epoxy composites for lightweight structural applications.

DOI: 10.15376/biores.21.2.4792-4809

Keywords: Pineapple leaf fiber; Micromechanical; Tensile; Flexural; RVE

Contact information: a: School of Mechanical Engineering, VIT-AP University, Besides A.P. Secretariat, Amaravati 522237, Andhra Pradesh, India; b: Department of Industrial Engineering, College of Engineering, Imam Mohammad Ibn Saud Islamic University (IMSIU), Riyadh 11432, Saudi Arabia; c: Faculty of Artificial Intelligence and Engineering, Multimedia University, 63100 Cyberjaya, Malaysia; d: Centre for Smart Systems and Automation, COE for Robotics and Sensing Technologies, Multimedia University, 63100 Cyberjaya, Malaysia; e: Centre for Electric Energy and High Voltage Engineering (CEEHVE), COE for Robotics and Sensing Technologies, Multimedia University, 63100 Cyberjaya, Malaysia; f: Engineering Sciences Research Center (ESRC), Deanship of Scientific Research, Imam Mohammad Ibn Saud Islamic University (IMSIU), Riyadh 11432, Saudi Arabia;
** Corresponding authors: sksahumech@gmail.com; ielee@mmu.edu.my*

INTRODUCTION

In today's world, sustainability has become a key priority, prompting industries to seek eco-friendly alternatives. Natural fibers have emerged as a strong contender due to their numerous benefits, including relatively low density, biodegradability, and low cost. Natural fibers play a crucial role in reducing carbon footprints and addressing the growing issue of plastic waste, often caused by synthetic fibers (Carranza-Nuñez *et al.* 2021; Rahaman and Moshwan 2026). Natural fibers in epoxy matrices can provide flexibility and structural integrity. Epoxy, a strong and durable polymer, enhances the strength and versatility of natural fibers, resulting in a composite material that is both lightweight and highly durable (Mahmud *et al.* 2025; Gani *et al. 2024*). Evaluating the mechanical

properties of these composites is essential to determine their strength, durability, and performance, ensuring their suitability for a wide range of industrial applications, including construction, automotive, sports, and biomedical applications (Namvar *et al.* 2014; Khan *et al.* 2018).

There are several literature articles that provide insight into the mechanical properties of epoxy/natural fiber epoxy composites. Mechanical properties of basalt fiber fabric epoxy composite at 50, 55, and 60 wt% was successfully fabricated (Kiran *et al.* 2025). It was observed that, among all samples, the 60 wt% basalt fiber composite demonstrated superior flexural strength and modulus, increasing by 10.9% and 6.9% compared to pure epoxy. Mohammed *et al.* (2025) examined the mechanical properties of the bamboo fiber/epoxy composite with varying fiber loading (9 to 18 wt%). It was observed that the highest tensile strength was noted at 13.5 wt% of fiber loading. Mishra *et al.* (2025) studied four types of agro residue fibers (*i.e.*, paddy straw, bagasse, mustard stalk, and wood sawdust) in epoxy composites. The results showed that paddy straw outperformed bagasse by 17%, mustard stalk by 19%, and wood sawdust by 35% in tensile strength. A study by Pramanik *et al.* (2024) focused on fabricating a jute-epoxy composite with 52.5% jute and 47.5% epoxy resin using manual lay-up. The composite achieved a tensile strength of 42.91 MPa and a bending strength of 69.3 MPa, with numerical analysis validating the experimental results. Akhyar *et al.* (2024) investigated the effect of coconut fiber lengths (2, 4, and 6 mm) on the flexural strength of a coconut fiber epoxy composite. The results showed that while fiber length influenced flexural strength, the variation was minimal, with the highest flexural strength of 10.7 MPa observed for the 6 mm fiber composite. Shahapurkar *et al.* (2024) studied the flexural behaviour of banana fiber-reinforced epoxy composites with different architectures, *i.e.*, chopped and woven fibers, both treated and untreated. It was seen that the treated woven banana epoxy composite (TWBEC) exhibited 11 to 25% higher flexural strength than other composites, with numerical simulation and experimental results showing good agreement. A study by Tadese *et al.* (2025) investigated the effects of climate, alkali treatment, and fiber loading on the mechanical properties of sisal fiber-epoxy composites. Results showed that alkali treatment improved properties, with sisal fibers from dry climates exhibiting up to 161% higher tensile strength and 65% higher flexural strength at 40% fiber loading than those from humid climates. Husham *et al.* (2025) showed that an epoxy composite reinforced with 5% calcined eggshell powder and 20% millet stalk fibers exhibited the highest tensile strength of 60 MPa and flexural strength of 89.4 MPa among all samples. A study by Sangamesh *et al.* (2024) investigated areca leaf-reinforced epoxy composites prepared using NaOH-treated and untreated fibers at varying weight fractions (35 and 45 wt%). Results showed that untreated composites with 45% fiber content achieved the highest tensile strength (39 MPa). Kurien *et al.* (2024) explored the impact of the arrangement of jute-vetiver fiber-reinforced epoxy composites. Specimen 3, with a sandwich structure of jute and vetiver layers, exhibited enhanced mechanical properties, including a 25.4% improvement in tensile strength and a 56.7% improvement in flexural strength. Singh and Hirwani (2023) conducted a study using an epoxy matrix, reinforced with *Saccharum munja* fibers at volume fractions of 10 to 25%. The 20% fiber composite exhibited the best mechanical properties, with tensile and flexural strengths of 110 and 130 MPa, respectively, while a 25% fiber content resulted in reduced performance. Wagh *et al.* (2025) reported that flax fiber–reinforced epoxy composites showed ~90% higher tensile strength and ~17% higher flexural strength than sisal fiber composites, achieving 205 MPa tensile strength, 158 MPa flexural strength, and 45 J energy absorption. Sarikaya *et al.*

(2019) investigated epoxy composites reinforced with birch, palm, and eucalyptus fibers, fabricated using resin transfer moulding and moulded fiber techniques. Mechanical testing showed that fiber type strongly affected performance: tensile strengths were 29.5 MPa (birch), 42.2 MPa (palm), and 45.3 MPa (eucalyptus); flexural strengths were 58.8 MPa, 68.6 MPa, and 79.9 MPa, respectively. The study confirmed that moulded fiber production effectively enhances natural fiber–epoxy composite properties.

Although extensive studies have been reported on the mechanical behaviour of natural fiber–reinforced epoxy composites using basalt, bamboo, jute, and coconut fibers, investigations focusing on pineapple leaf fiber (PALF)–epoxy systems remain limited. PALF is an attractive reinforcement owing to its biodegradability, high tensile strength, and superior strength-to-weight ratio. Moreover, the application of Finite Element Method (FEM)–based Representative Volume Element (RVE) modeling to predict the mechanical response of PALF-reinforced epoxy composites is still underexplored in the literature. The novelty of the present work lies in the combined experimental–numerical approach, wherein tensile and flexural behaviors of PALF/epoxy composites are systematically evaluated across varying fiber loadings using both laboratory testing and FEM-based RVE simulations. This integrated methodology enables accurate prediction of mechanical performance while minimizing material consumption during experimentation and reducing overall testing cost, thereby offering a more efficient framework for the design and analysis of PALF-reinforced epoxy composites.

EXPERIMENTAL

Materials

The epoxy resin (LY 556) was sourced from Herenba Instruments & Engineering Ltd., Chennai, India. The density of epoxy and hardeners ranges from 1.15 to 1.20 g/cm³. The pineapple leaf fiber (PALF) has an average fiber length between 30 and 50 mm and a moisture content of less than 10%. Sourced from the local vendor Vijayawada, India. The properties of materials are shown in Table 1.

Table 1. Properties of PALF

Properties	Value
Density (g/cm^3)	1.07
Tensile strength (MPa)	126.60
Young's modulus (MPa)	4405
Elongation at break (%)	2.2

Micromechanical Models

Rule of mixture

The rule of mixtures is the most commonly used fundamental micromechanical approach for estimating the properties of composite materials based on the properties and volume fractions of a weighted average of the individual materials, such as fiber and epoxy. The assumption underlying this method is that the phases of both the epoxy and the fiber should be uniformly distributed and well-bonded. In the two-phase composite system, the effective modulus of the epoxy composite can be expressed as Eqs. 1 and 2 (Rathod *et al.* 2026),

$$P_c = V_f E_f + V_m E_m \quad (1)$$

$$V_f + V_m = 1 \quad (2)$$

where E_f (Pa) and E_m (Pa) are the effective modulus of the fiber and matrix, respectively, and V_f and V_m are their corresponding volume fractions.

Mori-Tanaka model

The Mori-Tanaka approach was used to predict the mechanical properties of composite materials. The effective properties of the composite were calculated based on the individual properties of the phases and their volume fractions. The Mori-Tanaka model's mean-field approximation was applied to estimate the effective modulus properties (C_E) of the composite system, assuming isotropic inclusions embedded in a matrix as shown in Eq. 3 (Sundarasetty and Sahu 2025),

$$C_E = M_E \left[\frac{\left(1+\frac{f_v}{1-f_v}\right)+3\left(\frac{1-f_v}{M_E+\left(\frac{1-f_v}{f_E}\right)}\right)}{\left(1+\frac{f_v}{1-f_v}\right)-3\left(\frac{1-f_v}{M_E+\left(\frac{1-f_v}{f_v}\right)}\right)} \right] \quad (3)$$

where C_E, M_E, f_E are the modulus values of the composite (Pa), matrix (Pa), and fiber (Pa), respectively, and f_v is the fiber volume fraction.

Composite Fabrication

Figure 1(a) provides a comprehensive overview of the fabrication route adopted for preparing PALF–epoxy composite laminates, highlighting each critical processing step that influences the final composite quality.

Initially, bidirectional pineapple leaf fiber (PALF) fabrics were collected and vacuum-dried to remove absorbed moisture, as moisture can adversely affect fiber–matrix interfacial bonding and lead to void formation during curing. Subsequently, the epoxy resin and hardener were mixed in a 10:1 weight ratio, following the manufacturer's recommendations, and stirred vigorously for 3 to 5 min to ensure a homogeneous resin system with uniform curing characteristics. Prior to composite lay-up, a releasing agent was applied to the mold surface to facilitate easy demolding and prevent surface damage to the cured laminate.

The bidirectional PALF fabric was then carefully positioned inside the mold to maintain fiber alignment and structural integrity. The epoxy–hardener mixture was uniformly applied using a squeegee to promote complete fiber wetting, minimize air entrapment, and enhance resin penetration through the fiber network.

After lay-up, the laminate was cured at room temperature for 24 h to allow initial crosslinking, followed by post-curing at 60 to 80 °C for 2 to 4 h to achieve complete resin curing and improved mechanical stability. Finally, the cured laminates were machined into standard tensile and flexural specimens according to ASTM D3039 (2017) and ASTM D790-03 (2017), as shown in Fig. 1(b) and Fig. 1(c) (Nagaraja et al. 2024; Nithiyapathi et al. 2026). The prepared specimens were designated as pure epoxy and PALF/epoxy composites containing 5%, 10%, 20% and 30% fiber loadings.

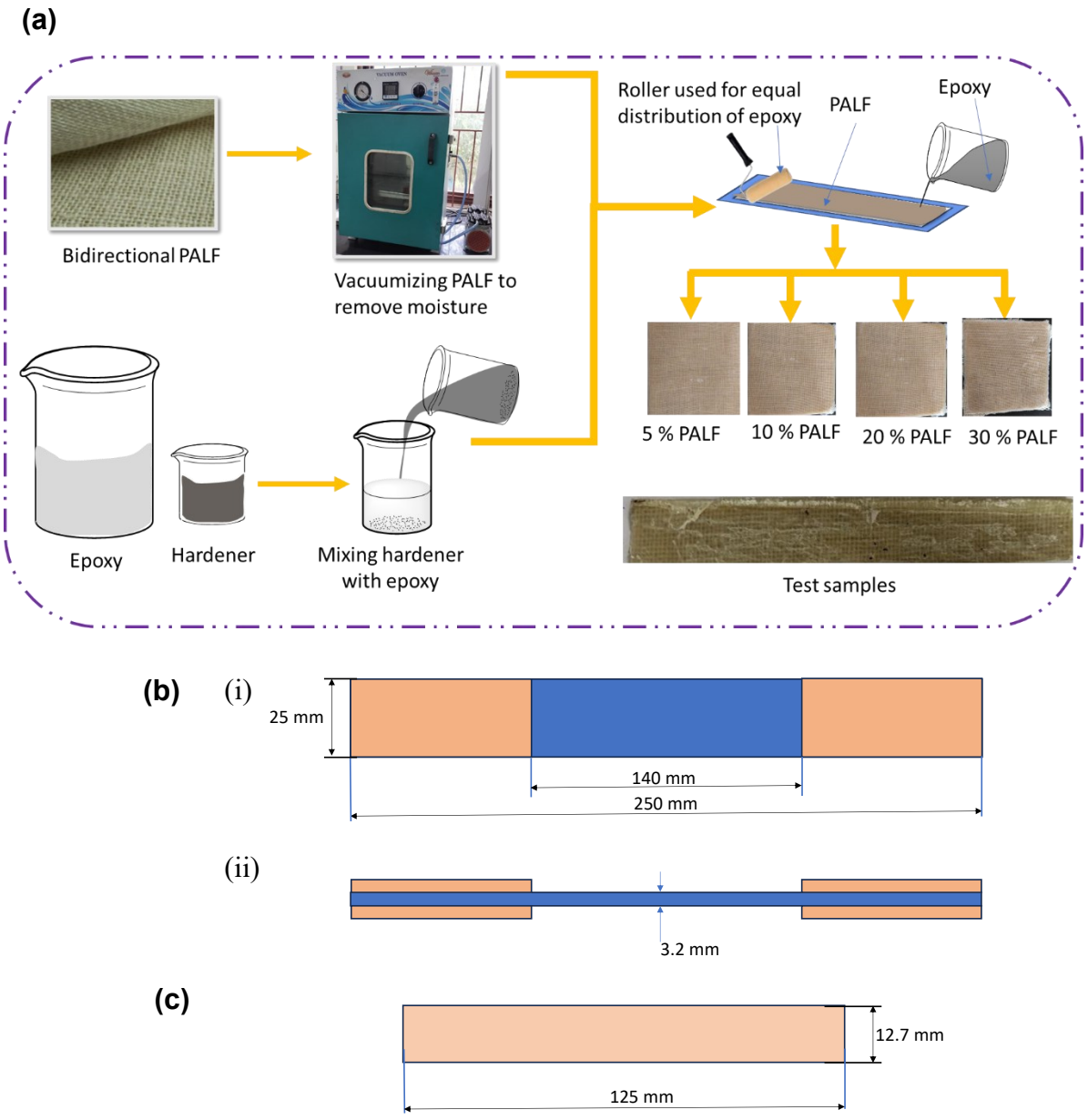

Fig. 1. a) Steps involved in sample fabrication, (b) tensile sample ASTM D3039 (2017) (i) top view, (ii) side view, (c) flexural sample ASTM D790-03 (2017)

Experimental Testing

Tensile tests were performed using a universal testing machine (UTM) (H10KL, Tinus Olsen India Pvt. Ltd., India) as per the ASTM D3039 (2017). A unidirectional load with a strain rate of 2 mm/min was applied under standard atmospheric conditions. Similarly, the flexural tests were performed under the same conditions as per the ASTM D790-03 (2017). Each test was repeated three times, and the average values were recorded.

Finite Element Analysis (FEA)

Finite Element Analysis (FEA) is a computational technique used to predict the behavior of PALF/epoxy composite materials under various loading conditions. For the PALF/epoxy composite, FEA is utilized in ANSYS Workbench v. 2019 R3

Material Design Through RVE

The RVE design of PALF/epoxy composite material was performed in the material design module of ANSYS Workbench v. 2019 R3. A convergent analysis was conducted to determine the optimal RVE dimensions for accurate results. The RVE was generated with dimensions of 2.85 x 2.85 x 0.4 micrometers to simulate the composite materials' elastic modulus across all samples. The RVE models were created for PALF/epoxy composite samples with varying PALF weight percentages (5, 10, 20, and 30), as illustrated in Figs. 2a through 2d. The material properties derived from the RVE analysis were then used in the ANSYS Workbench module for further analysis.

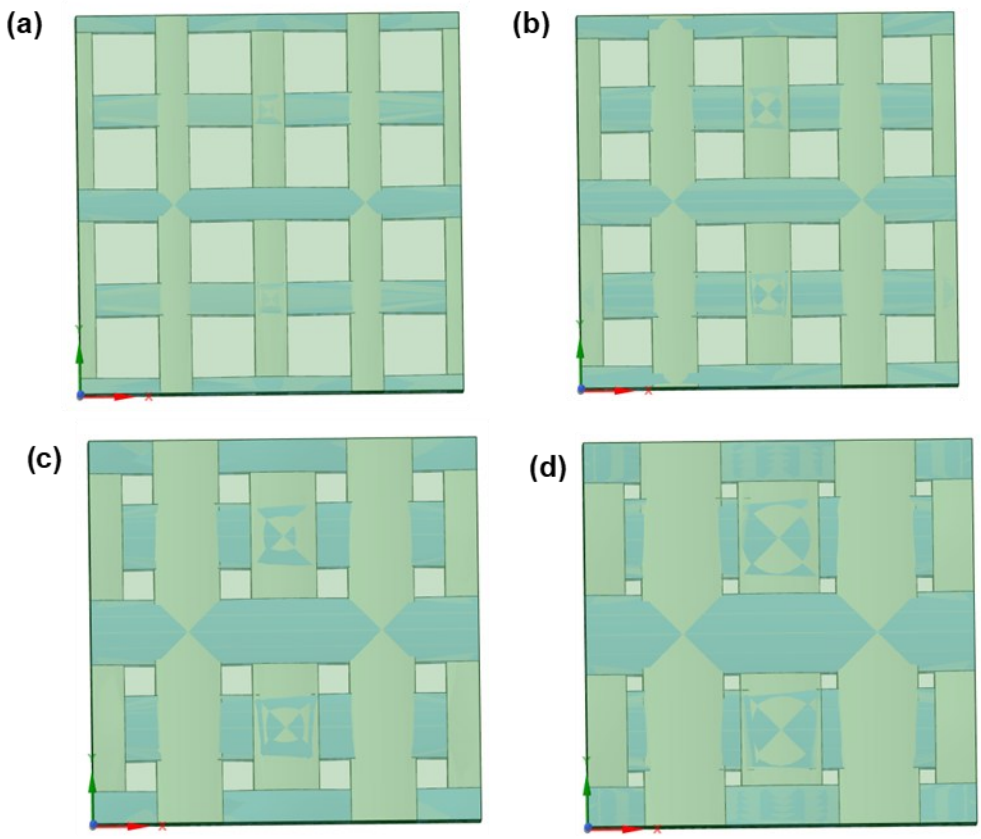

Fig. 2. RVE of a) 5% PALF/epoxy, b) 10% PALF/epoxy, c) 20% PALF/epoxy, and d) 30% PALF/epoxy composites

Tensile Strength Analysis

The Tensile strength analysis was performed in the static structural module of ANSYS Workbench on the tensile sample, per ASTM D3039 (2017). To perform the analysis, the tensile geometry was imported into the module, then assigned the material, which is designed using an RVE design module. The imported geometry was then discretized using a quad mesh with 8660 elements and 45611 nodes, as shown in Figs. 3a and 3b. The elements and node numbers were kept relatively uniform across all samples. The boundary condition was assigned by fixing the right side of the sample, while a load was applied to the other side in the positive x-direction, as shown in Fig. 3c. The load value used in the simulation corresponded to the ultimate load obtained from the experimental results, ensuring that the simulation accurately reflected the material's tensile behavior under applied conditions.

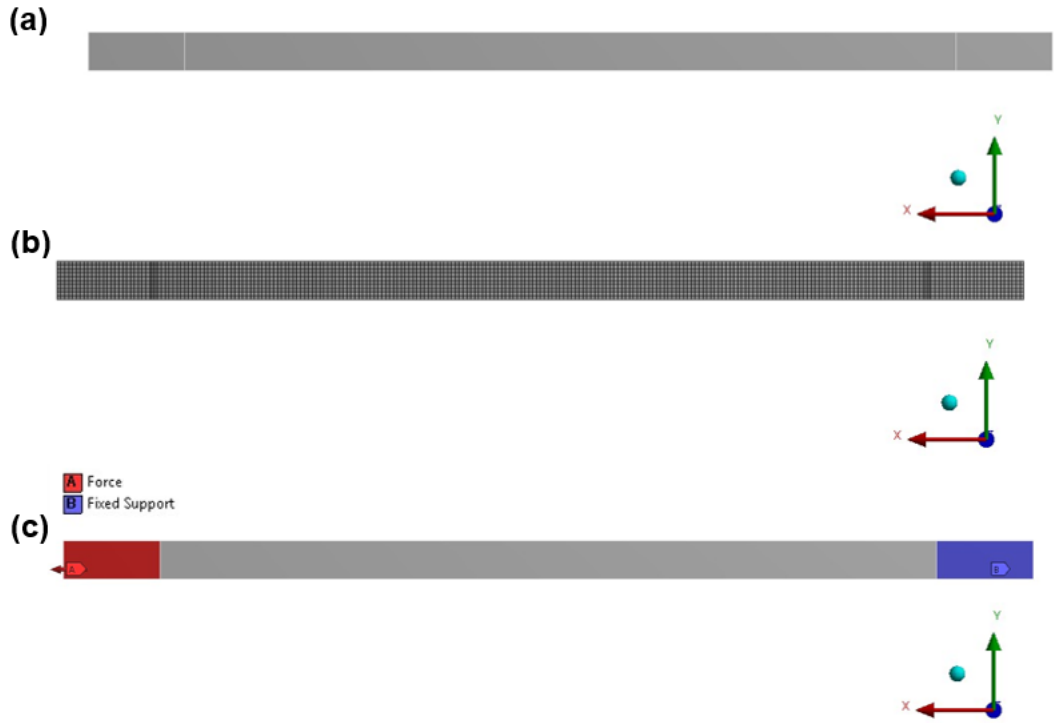

Fig. 3. a) Tensile sample, b) meshed view, and c) boundary conditions

Flexural Strength Analysis

The flexural strength analysis was performed in 3-point bending mode using the static structural module in ANSYS Workbench, following ASTM D790-03 (2017). To perform the analysis, the flexural geometry was first imported into the module, and then the RVE material design calculated composite values that were assigned. The imported flexural geometry was then meshed with 78260 elements and 345322 nodes, as shown in Figs. 4a and 4b. The elements and node numbers were kept uniform for all samples. The two cylinders at the lower part of the sample were constrained. Then, the load was applied through the cylinder at the top of the sample in the negative z-direction, as illustrated in Fig. 4c. The load value used in the simulation corresponded to the ultimate load obtained from the experimental results. This was to ensure that the simulation accurately reflected the material's flexural behavior under the applied conditions.

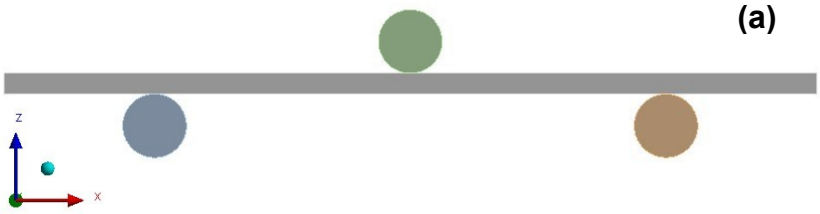

Fig. 4a. a) 3-point bending sample, b) meshed view, and c) boundary conditions

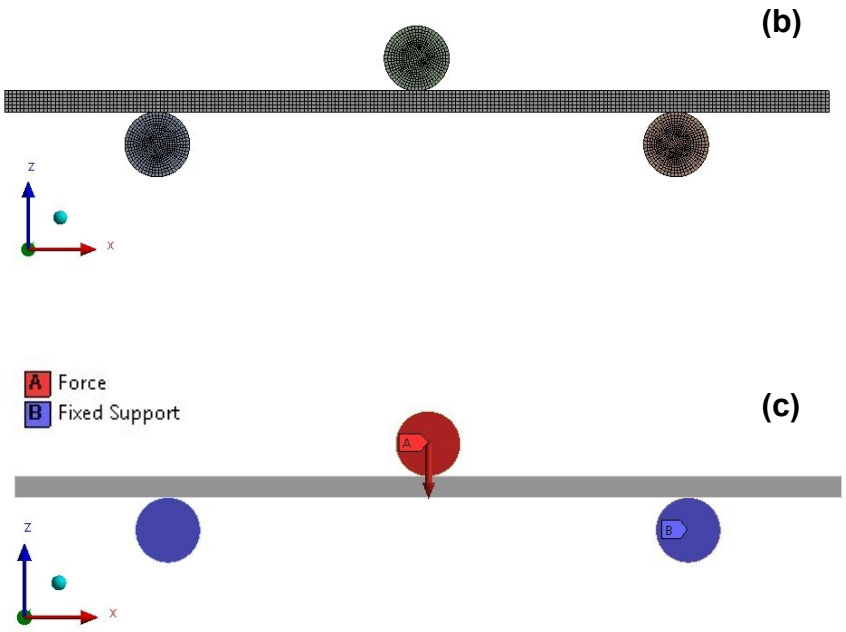

Fig. 4b & 4c. a) 3-point bending sample, b) meshed view, and c) boundary conditions

RESULTS AND DISCUSSION

Tensile Test

Figure 5a shows the stress-strain curve for pure epoxy along with 5%, 10%, 20%, and 30 wt% PALF/epoxy composite samples. The graph shows an increasing trend of peak stress with increase in fiber content. This indicates that load-resisting ability increased with fiber content. Figure 5b shows the tensile strength and Young's modulus results for all the samples, which was obtained from stress-strain curve. The results show that for pure epoxy (0% PALF), the tensile strength was 14.1 MPa, and the Young's modulus was 1280 MPa. When 5 wt% PALF was added to the epoxy matrix, the tensile strength increased by 10.6%, and Young's modulus increased by 5.8%. With 10% PALF, both properties were increased further, with tensile strength increasing by 60.3% and Young's modulus increasing by 10.1%. At 20% PALF, the composite became even more robust, with tensile strength increasing by 90% and Young's modulus increasing by 17.5%. At 30% PALF, the composite reached its peak performance, with tensile strength improving by 167.4% and Young's modulus increasing by 24% relative to the starting condition.

A moderate increase in fiber content enhanced the stiffness and strength of the epoxy composite due to effective load transfer from the matrix to the reinforcing fibers. The presence of fibers can promote a more uniform stress distribution within the epoxy matrix, thereby delaying crack initiation and reducing localized failure, which can result enhancement of tensile performance. Such reinforcing mechanisms have been widely reported for natural fiber–reinforced epoxy systems, where interfacial adhesion and fiber dispersion govern the strengthening effect (Khan *et al.* 2018; Mohammed *et al.* 2015; Sanjay *et al.* 2016). In addition, the increase in fiber content in the epoxy improves its resistance to deformation, which is reflected in the steady increase in Young's modulus. Figure 6 shows a comparison plot between the Young's modulus obtained from experimental *vs.* micromechanical models and the RVE model of PALF/epoxy composite. It was noted that for 5% PALF, the RVE model predicted a value 4.63% higher than the

experimental result, while the Rule of Mixture predicted 7.32% higher, and Mori-Tanaka showed a negligible error of just 0.03%. For 10% PALF, RVE had an 11.2% error, Rule of Mixture 15.4%, and Mori-Tanaka had a smaller 2.10% error. For 20% PALF, RVE showed a 2.17% error, Rule of Mixture 3.34%, and Mori-Tanaka had a larger error of 13.9%. Lastly, for 30% PALF, RVE predicted a 3.90% error, Rule of Mixture 4.9%, and Mori-Tanaka had a substantial 21.5% error. These variations highlight the models' showed good predictive capacity, with minor discrepancies.

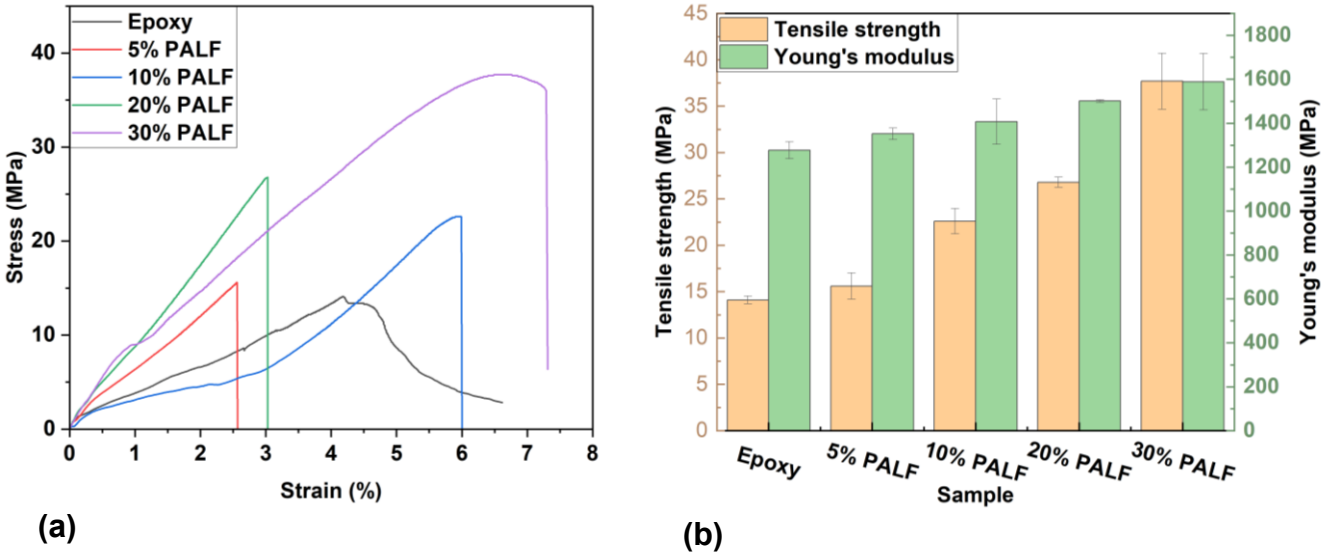

Fig. 5. a) Stress-strain curve for tensile test, b) tensile strength and Young's modulus *vs.* sample

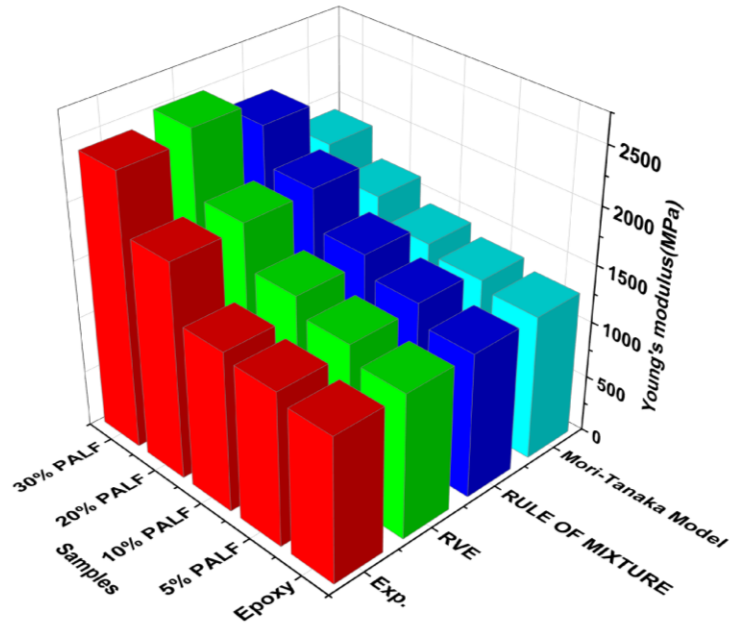

Fig. 6. Micromechanical models *vs.* experimental Young's modulus

Flexural Test

Figure 7(a) illustrates the flexural stress–strain responses of neat epoxy and PALF-reinforced epoxy composites, showing a clear increase in peak stress with increasing fiber content. The corresponding flexural strength values extracted from these curves are presented in Fig. 7(b). Neat epoxy (0 wt%) exhibited a flexural strength of 40.8 MPa, which is relatively modest and can be attributed to the brittle nature of the epoxy matrix and the absence of reinforcement. With the addition of 5 wt% PALF, the flexural strength increased by 10.1%, followed by 19.8% at 10 wt% PALF, indicating the initial contribution of fibers to load sharing under bending. A pronounced improvement is observed at 20 wt% PALF, with a 77.7% increase, suggesting more effective stress transfer between the fibers and matrix. At 30 wt% PALF, the flexural strength increased by 143%, reflecting fiber-dominated bending behaviour. Although the absolute flexural strength values were lower than those of synthetic fiber composites, similar ranges have been reported for untreated natural fiber–epoxy systems fabricated by manual lay-up, where interfacial efficiency and void content limit peak strength. Nevertheless, the substantial relative improvement confirms the effective reinforcing role of PALF in enhancing the flexural performance of the epoxy matrix. The increase in flexural strength with higher PALF content can be attributed to improved load transfer and the greater contribution of the stiff fiber phase (Patel *et al.* 2023; Marchi *et al.* 2024).

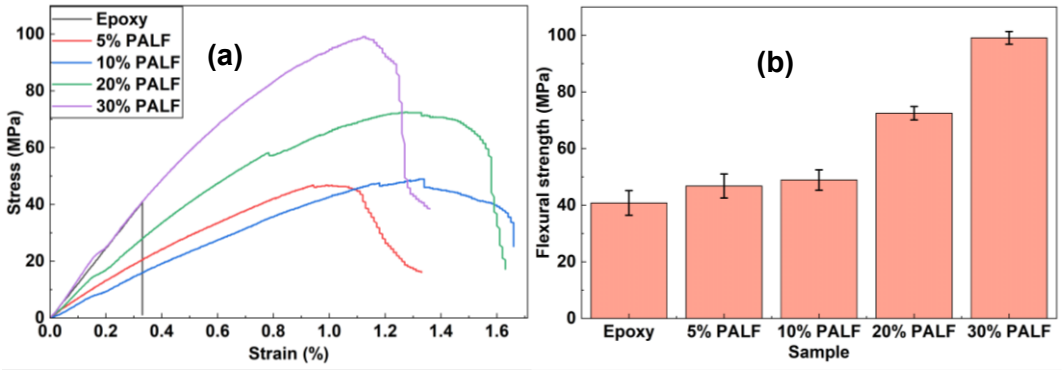

Fig. 7. a) Stress-strain curve for flexural test, b) flexural strength *vs.* samples

Finite Element Analysis

Tensile test

Figure 8a, 8b, 8c, 8d and 8e shows the stress contour map of the tensile specimen, providing insight into the stress distribution during the tensile test. The color gradient, ranging from blue (low stress) to red (high stress), represents the varying stress levels across the specimen. It is observed that the stress gradually increases from the fixed ends toward the center of the specimen. Notably, there is a concentration of high stress (red) near the holding points at both ends of the specimen, indicating localized stress due to the applied constraints, and afterwards, the stress distribution is more uniform toward the center. The results from Fig. 8a show that the stress contour map, which shows that for pure epoxy, the maximum stress value is predicted to be 14.6 MPa. The PALF/epoxy composite samples with 5%, 10%, 20%, and 30% PALF show an improvement of 10.1%, 47.1%, 72.7%, and 176.7% respectively as the fiber content is increased. Figure 9 shows the comparison between the experimental tensile strength results and the ANSYS simulation results. The errors between the simulation and experimental results for pure

epoxy and epoxy/PALF composites with different PALF contents (5% to 30%) were calculated. The percentage errors are 3.2%, 2.7%, 5.1%, 6.3%, and 6.5%, for 0%, 10%, 20%, and 30% PALF, respectively. These results demonstrate that the simulation and experimental errors were all below 10%, highlighting the simulation's accuracy and reliability in predicting the tensile behavior of the epoxy/PALF composites.

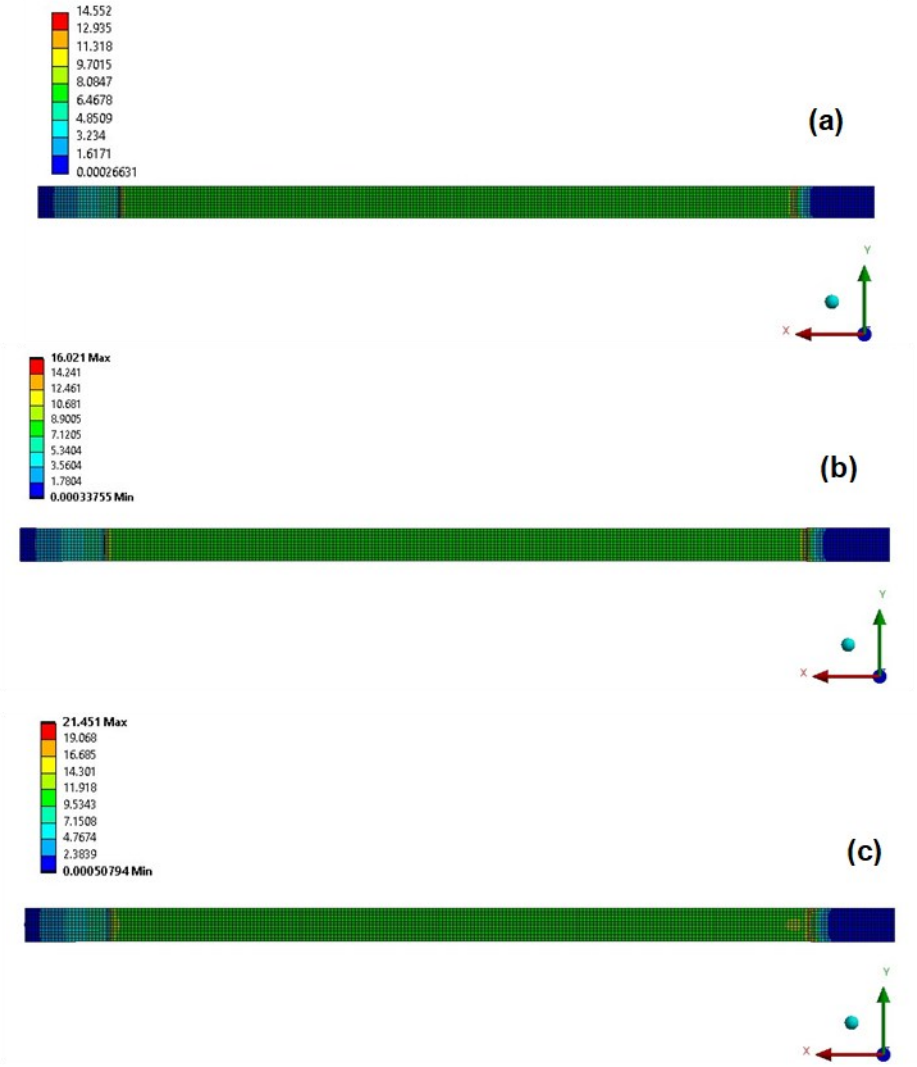

Fig. 8(a-c). Tensile stress contour map for a) epoxy, b) % PALF/epoxy, c) 10% PALF/epoxy, d) 20% PALF/epoxy, and e) 30% PALF/epoxy composites

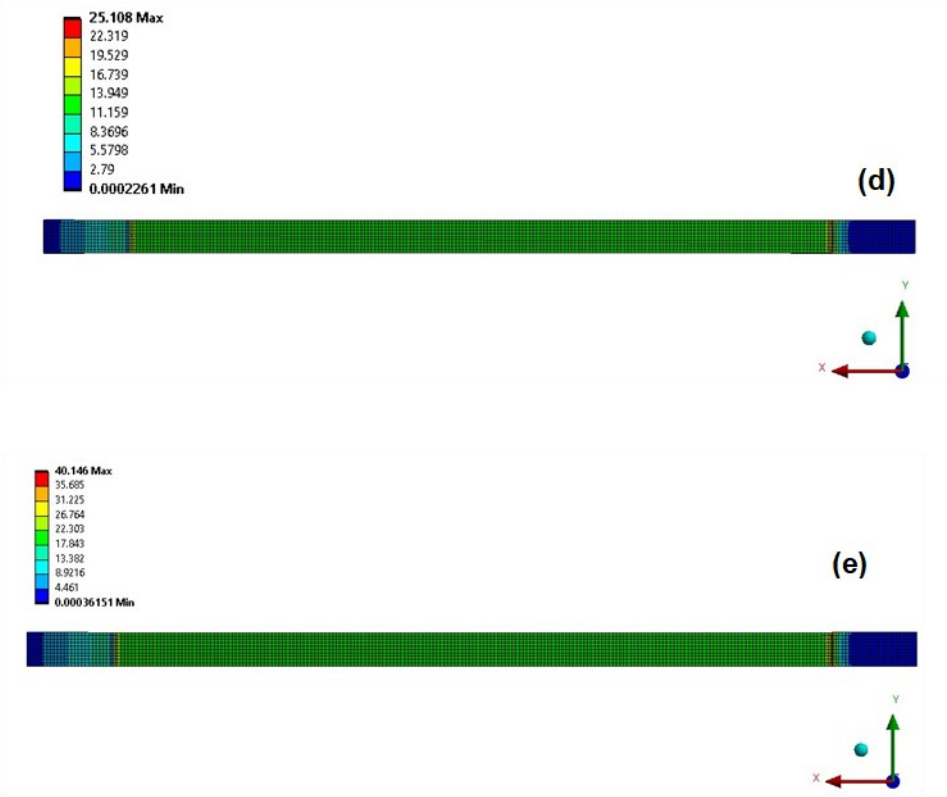

Fig. 8(d & e). Tensile stress contour map for a) epoxy, b) % PALF/epoxy, c) 10% PALF/epoxy, d) 20% PALF/epoxy, and e) 30% PALF/epoxy composites

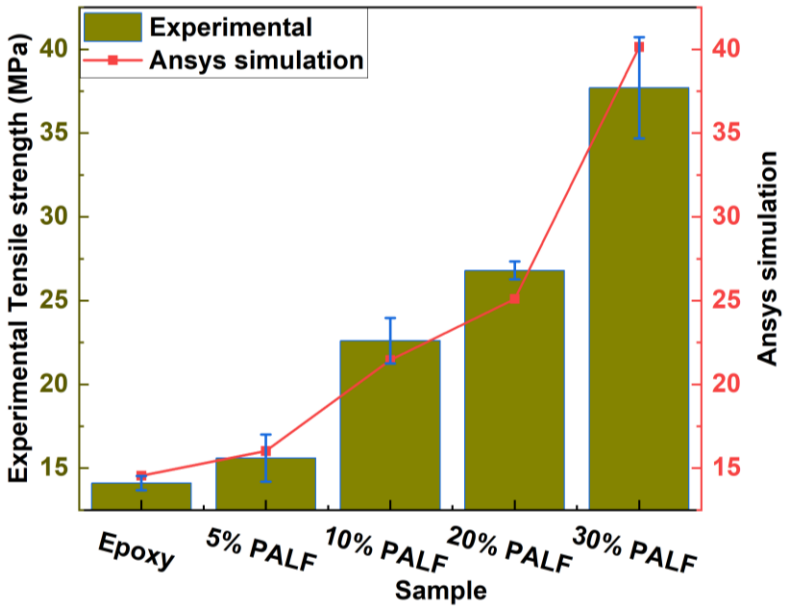

Fig. 9. Comparison plot of tensile strength from experimental and ANSYS simulation

Flexural test

Figures 10a through 10e show the flexural strength analysis stress contour map results for all specimens. The color gradient, ranging from blue (low stress) to red (high

stress), represents the distribution of stress across the specimen. This shows that the highest stress is concentrated near the middle, which is typical in flexural testing. The outer regions show much lower stress, as expected, because the material is less deformed near the supports. From the contour map of Fig. 10a, the maximum stress for pure epoxy is 39.1 MPa. As shown in Fig. 10b for the 5% PALF composite, the maximum stress increases to 44.9 MPa, representing a 14.8% improvement over pure epoxy. As shown in Fig. 10c for 10% PALF, the maximum stress further increases to 47.2 MPa, with a 20.7% increase over the pure epoxy. As shown in Fig. 10d for 20% PALF, the maximum stress increases to 70.8 MPa, indicating a substantial 50.2% improvement over pure epoxy. As shown in Fig. 10e for 30% PALF, the composite achieves a maximum stress of 96.9 MPa, representing a substantial 147% increase over pure epoxy. These results demonstrate that the addition of PALF fibers enhances flexural strength and bending resistance, with the highest performance observed at 30% PALF. Figure 11 shows a comparison of the experimental and simulated results for the flexural test. The percentage errors for pure epoxy and 5%, 10%, 20%, and 30% PALF/epoxy composites are 4%, 4%, 3%, 2%, and 2%, respectively. The results highlight the accuracy of the ANSYS simulation in predicting the flexural strength of the composites.

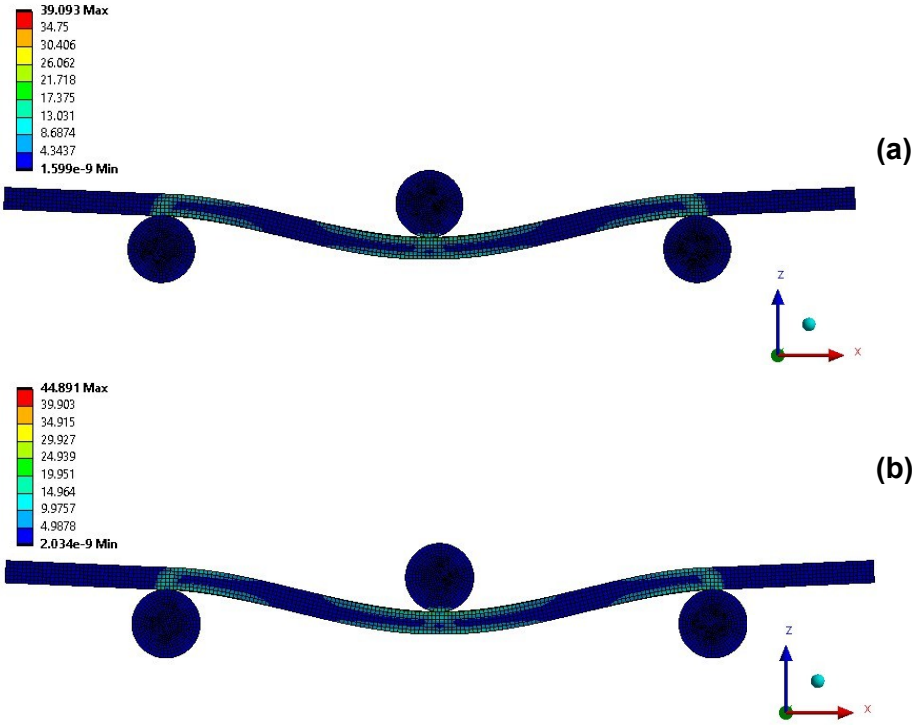

Fig. 10(a & b). Flexural stress contour map for a) epoxy, b) 5% PALF/epoxy, c) 10% PALF/epoxy, d) 20% PALF/epoxy, and e) 30% PALF/epoxy composites

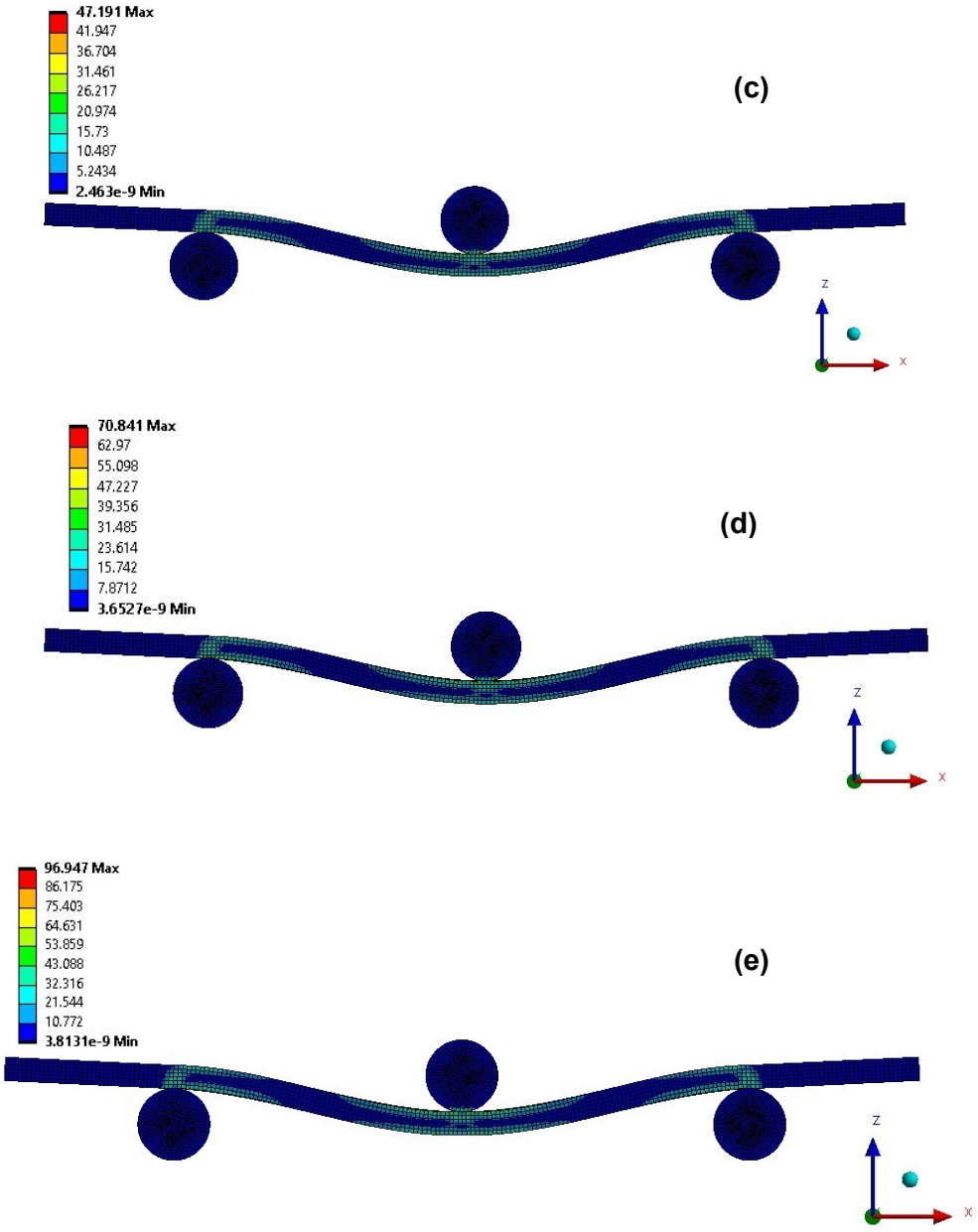

Fig. 10(c – e). Flexural stress contour map for a) epoxy, b) 5% PALF/epoxy, c) 10% PALF/epoxy, d) 20% PALF/epoxy, and e) 30% PALF/epoxy composites

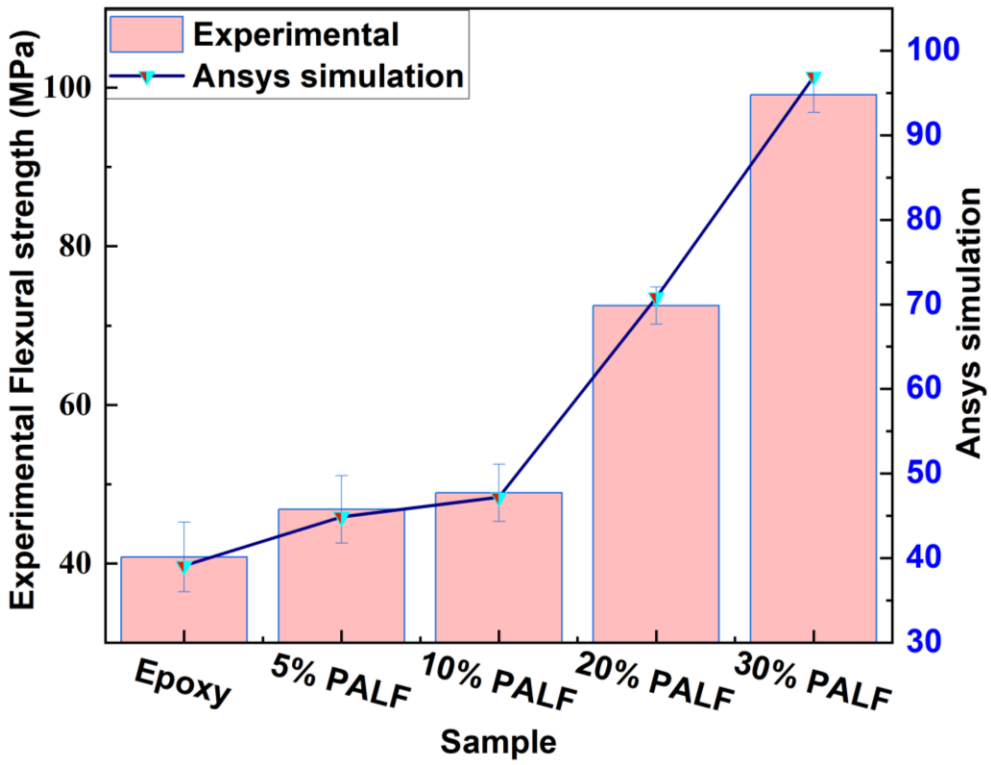

Fig. 11. Comparison plot of flexural strength from experimental and ANSYS simulation

CONCLUSIONS

The study demonstrated that reinforcing an epoxy matrix with pineapple leaf fiber (PALF) significantly improved its mechanical performance. Both RVE-based modeling and FEA accurately predicted the composite's stiffness and strength, showing good agreement with experimental results and established micromechanical models. These findings highlight the effectiveness of combining natural fiber reinforcement with computational modeling for designing high-performance epoxy composites.

ACKNOWLEDGEMENTS

Funding

This work was supported and funded by the Deanship of Scientific Research at Imam Mohammad Ibn Saud Islamic University (IMSIU) (grant number IMSIU-DDRSP2603).

Data Availability Statement

The original contributions presented in this study are included in the article.

REFERENCES CITED

Alnada Faris Husham, K., Khdier, H. M., and Salih, W. M. (2025). "Eco-friendly epoxy composites for high-performance skateboards," *Discover Materials* 5(1), article 186. https://doi.org/10.1007/s43939-025-00354-z

ASTM D3039/D3039M-17 (2017). "Standard test method for tensile properties of polymer matrix composite materials," ASTM International, West Conshohocken, PA, USA. https://doi.org/10.1520/D3039_D3039M-08

ASTM D790-03 (2017). "Standard test methods for flexural properties of unreinforced and reinforced plastics and electrical insulating materials," ASTM International, West Conshohocken, PA, USA. https://doi.org/10.1520/D0790-03

Carranza-Nuñez, U., Ramiro Vasquez-Garcia, S., Flores-Ramirez, N., Ahmed Abdel-Gawwad, H., Luis Rico, J., Arizbe Santiago, A., Vargas, J., and Cruz-de-Leon, J. (2021). "Physicochemical characterization of natural fibers obtained from seed pods of *Ceiba aesculifolia*," *BioResources* 16(2), 4200-4211. https://doi.org/10.15376/biores.16.2.4200-4211

Gani, A., Ibrahim, M., Ulmi, F., and Farhan, A. (2024). "The influence of different fiber sizes on the flexural strength of natural fiber-reinforced polymer composites," *Results in Materials* 21, article 100534. https://doi.org/10.1016/j.rinma.2024.100534

Khan, M. Z., Srivastava, S. K., and Gupta, M. K. (2018). "Tensile and flexural properties of natural fiber reinforced polymer composites: A review," *J. Reinf. Plast. Compos.* 37(24), 1435-1455. https://doi.org/10.1177/0731684418799528

Kiran, R., Prakash, K. R., and Suresha, B. (2025). "Experimental investigations on the mechanical behavior of basalt fabric reinforced epoxy composites," *J. Polym. Res.* 32(3), article 112. https://doi.org/10.1007/s10965-024-04123-x

Kurien, R. A., Kannan, G., Kurup, G. B., Reji, G. S., Santhosh, A., Paul, D., Rangappa, S. M., Suttiruengwong, S., and Siengchin, S. (2024). "Comparative mechanical and morphological characteristics of an innovative hybrid composite of vetiver and jute," *J. Polym. Res.* 31(12), article 356. https://doi.org/10.1007/s10965-024-04082-x

Mahmud, M. Z. A., Rabbi, S. F., Islam, M. D., and Hossain, N. (2025). "Synthesis and applications of natural fiber-reinforced epoxy composites: A comprehensive review," *SPE Polymers* 6(1), article e10161. https://doi.org/10.1002/pls2.10161

Marchi, B. Z., da Silveira, P. H. P. M., Almeida Bezerra, W. B., da Silva, M. H. P., Monteiro, S. N., and da Silva Figueiredo, A. B. H. (2024). "Evaluation of the thermomechanical properties of novel epoxy composites reinforced with *Geonoma baculifera* fibers," *Scientific Reports* 14(1), article 26565. https://doi.org/10.1038/s41598-024-78449-5

Mishra, D. K., Singh, B. R., Kumar, S., Sharma, V. K., and Singh, N. (2025). "Design and optimization of agro-residue fiber-reinforced composite panels for sustainable grain storage," *Fibers Polym.* 26(11), 5023-5038. https://doi.org/10.1007/s12221-024-06892-y

Mohammed, K., Zulkifli, R., Tahir, M. F. M., Gaaz, T. S., and Salih, A. A. (2025). "Optimization of fiber parameters for the mechanical strength of bamboo fiber/epoxy composites using central composite design," *Results Eng.* 31, article 105414. https://doi.org/10.1016/j.rineng.2025.105414

Mohammed, L., Ansari, M. N., Pua, G., Jawaid, M., and Islam, M. S. (2015). "A review on natural fiber reinforced polymer composite and its applications," *International*

Journal of Polymer Science 2015, article 243947. https://doi.org/10.1155/2015/243947

Nagaraja, S., Anand, P. B., Shivakumar, H. D., and Ammarullah, M. I. (2024). "Influence of fly ash filler on the mechanical properties and water absorption behaviour of epoxy polymer composites reinforced with pineapple leaf fiber for biomedical applications," *RSC Adv.* 14(21), 14680-14696. https://doi.org/10.1039/D4RA00529E

Namvar, F., Jawaid, M., Tanir, P. M., Mohamad, R., Azizi, S., Khodavandi, A., Rahman, H. S., and Nayeri, M. D. (2014). "Potential use of plant fibers and their composites for biomedical applications," *BioResources* 9(3), 5688-5706. https://doi.org/10.15376/biores.9.3.5688-5706

Nithiyapathi, C., Manivannan, S., and Kavimani, V. (2026). "Synergistic enhancement of dynamic and thermo-mechanical properties of epoxy/glass fiber composites with GNP-MH fillers," *J. Polym. Res.* 33(1), article 7. https://doi.org/10.1007/s10965-025-04210-9

Patel, R. V., Yadav, A., and Winczek, J. (2023). "Physical, mechanical, and thermal properties of natural fiber-reinforced epoxy composites for construction and automotive applications," *Applied Sciences* 13(8), article 5126. https://doi.org/10.3390/app13085126

Pramanik, T. J., Rafiquzzaman, M., Karmakar, A., Nayeem, M. H., Turjo, S. K. S., and Abid, M. R. (2024). "Evaluation of mechanical properties of natural fiber based polymer composite," *BenchCouncil Trans. Benchmarks, Stand. Eval.* 4(3), article 100183. https://doi.org/10.1016/j.tbench.2024.100183

Rahaman, M. T., and Moshwan, M. M. (2026). "Advancements in natural fibers for sustainable textile manufacturing: Importance, sources, applications, and future prospects," *Next Materials* 10, article 101564. https://doi.org/10.1016/j.nxmate.2025.101564

Rathod, P., Washimkar, D., Anerao, P., Pawar, A., Yelamasetti, B., Patil, N., Sharma, S., Shelare, S., and Ramaswamy, K. (2026). "Homogenization technique-based prediction of elastic properties in pistachio shell powder-acrylic butadiene styrene (ABS) polymeric composites," *Polym. Polym. Compos.* 34, article 09673911251410749. https://doi.org/10.1177/09673911251410749

Sangamesh, R., Hiremath, S., Biradar, S., Kumar B, S., Sondar, P., and Vishwanatha, H. M. (2024). "Effect of alkaline treatment on mechanical properties of natural fiber-reinforced composite," *J. Mech. Sci. Technol.* 38(12), 6597-6605. https://doi.org/10.1007/s12206-024-1105-z

Sanjay, M., Arpitha, G., Naik, L. L., Gopalakrishna, K., and Yogesha, B. (2016). "Applications of natural fibers and its composites: An overview," *Natural Resources* 7(3), 108-114. https://doi.org/10.4236/nr.2016.73011

Sarikaya, E., Çallioğlu, H., and Demirel, H. (2019). "Production of epoxy composites reinforced by different natural fibers and their mechanical properties," *Composites Part B: Engineering* 167, 461-466. https://doi.org/10.1016/j.compositesb.2019.03.020

Shahapurkar, K., MC, K., Chenrayan, V., Kanaginahal, G., Gebremaryam, G., Nik-Ghazali, N. N., Kuan, T. M., Ariffin, A. M., Arunachalam, A., Fouad, Y., and Soudagar, M. E. M. (2024). "Flexural behavior of epoxy composites reinforced with banana fibers in different architectures: Experimental, analytical, and numerical approaches," *Biomass Convers. Biorefin.* 14(17), 21603-21618. https://doi.org/10.1007/s13399-024-05872-z

Singh, S. P., and Hirwani, C. K. (2023). "Mechanical and dynamic characterization of *Saccharum munja* fiber-reinforced epoxy composite," *J. Inst. Eng. India Ser. C* 104(6), 1181-1192. https://doi.org/10.1007/s40032-023-00982-x

Sundarasetty, H., and Sahu, S. K. (2025). "Experimental and computational study on the tensile and flexural properties of polylactic acid filled with boron nitride nanoplatelets," *Fract. Struct. Integr.* 19(72), 211-224. https://doi.org/10.3221/IGF-ESIS.72.16

Tadese, Y., Ayane, D., and Lemu, H. G. (2025). "Comparative study of influence of climatic conditions on physio-mechanical properties of sisal fibers and fiber-epoxy composites," *Results in Materials* 22, article 100769. https://doi.org/10.1016/j.rinma.2025.100769

Wagh, J. P., Malagi, R. R., and Madgule, M. (2025). "Investigative studies on natural fiber reinforced composites for automotive bumper beam applications," *J. Reinf. Plast. Comp.* 44(23-24), 2524-2534. https://doi.org/10.1177/07316844241285091

Article submitted: January 16, 2026; Peer review completed: February 21, 2026; Revised version received: February 28, 2026; Accepted: March 17, 2026; Published: April 16, 2026.
DOI: 10.15376/biores.21.2.4792-4809